Available online at www.sciencedirect.com
ScienceDirect
Trans. Nonferrous Met. Soc. China 27(2017) 2096−2103
Transactions of Nonferrous Metals Society of China
www.tnmsc.cn

Effect of cooling ways on properties of Al/Pb−0.2%Ag rolled alloy for zinc electrowinning

Xiang-yang ZHOU[1], Shuai WANG[1], Juan YANG[1], Zhong-cheng GUO[2,3], Jian YANG[2], Chi-yuan MA[1], Bu-ming CHEN[2]

1. School of Metallurgy and Environment, Central South University, Changsha 410083, China;
2. Faculty of Metallurgical and Energy Engineering, Kunming University of Science and Technology, Kunming 650093, China;
3. Kunming Hendera Science and Technology Co., Ltd., Kunming 650106, China

Received 17 May 2016; accepted 19 September 2016

Abstract: In order to study the new anode materials for zinc electrowinning, Al/Pb−0.2%Ag rolled alloy was produced by composite casting and hot rolling. Then the effect of cooling ways on properties of Al/Pb−0.2%Ag rolled alloy was investigated. As the results of metallographic test indicated, with the increasing of cooling intensity, both Vickers hardness and yield strength of Al/Pb−0.2%Ag rolled alloy increase. Furthermore, the Al/Pb−0.2%Ag rolled alloy, cooled by ice salt, presents the finest grain size and shows the lowest oxygen evolution potential (1.5902 V), while that of alloy cooled by water and air are 1.6143 V and 1.6288 V, respectively. However, the corrosion current density and corrosion rate of the Al/Pb−0.2%Ag rolled alloy, cooled by ice salt, are the highest. This can be attributed to its largest specific surface area, which promotes the contact between the anode and electrolyte.

Key words: Al/Pb−0.2%Ag rolled alloy; cooling way; electrocatalytic activity; electrochemical property; corrosion resistance; zinc electrowinning

1 Introduction

Over the past few decades, electrowinning has emerged as the preferred method for the final recovery of metals such as copper, zinc, nickel, manganese, and cobalt. Nearly 20% of the world's copper and more than 85% of the world's zinc are produced by hydro-electrometallurgical processes [1]. In the zinc-electrowinning industry, the Pb−(0.5%−1.0%)Ag anode is widely used because of its high corrosion resistance and high-stability in acidic sulfate solutions [2,3]. As an alloying element, the addition of silver can improve the conductivity, mechanical properties and corrosion resistance of lead anode [4,5]. Although the electro-chemical property, corrosion resistance and current efficiency of the ternary alloys (Pb−Ag−Ca, Pb−Ag−Ti, Pb−Ag−Sb, Pb−Ag−Sn, Pb−Ag−RE) and the quaternary alloys (Pb−Ag−Ca−Sr, Pb−Ag−Ca−Ce, Pb−Ag−Sn−Co) were researched and some valuable results have been obtained [6], those anodes can not effectively reduce the silver content of alloy. For the past few years, lead-based composite anodes containing active material such as WC, MnO_2, and PANI particles [7−9], electrodeposited MnO_2 and PbO_2 layer have exhibited superior electro-catalytic activity for oxygen evolution and excellent corrosion resistance in the zinc electrowinning. Unfortunately, the service life of those composite anodes is rather short due to the poor adhesion between substrate and the anodic deposited layer after a long time electrolysis in sulfuric acid based solution.

In recent years, aluminum substrate lead alloy anode has been widely studied [10−13]. Aluminum has good mechanical properties and low prices, which can significantly increase the mechanical strength of lead silver alloy anodes and reduce their production cost. Aluminum substrate lead alloy anode has a good application prospect in zinc electrowinning industry [14−17]. Different cooling ways will cause significant changes in microstructure morphology of solid state alloy [18]. Speeding up the cooling rate of alloy can refine grain size of alloy and change the alloy's

Foundation item: Projects (YNJJ2016012) supported by the Guangdong Jiana Energy and Technology Co., Ltd-Central South University Joint Research Funding, China
Corresponding author: Juan YANG; Tel/Fax: +86-731-88836329; E-mail: 646872865@qq.com
DOI: 10.1016/S1003-6326(17)60235-8

mechanical properties. At present, the effect of cooling methods on the properties of alloy have been investigated in many studies [19−23]. However, most of these studies are concentrated on aluminum or magnesium alloy. As far as we know, the grain size and mechanical properties of lead−silver alloy have remarkable effects on zinc electrowinning process, and there is no report about the effect of cooling ways on properties of lead−silver alloy.

Therefore, in this work, the effect of cryogenic cooling on the properties of lead−silver alloy are researched for the first time. Metallography test is used to inspect the microstructure of the alloy samples. The mechanical properties of alloy are measured by hardness and yield strength test. The electrochemical properties of different alloy samples are measured by anodic polarization curves (LSV), cyclic voltammetry curves (CV), Tafel curves and electrochemical impedance spectroscopy (EIS).

2 Experimental

2.1 Preparation of Al/Pb−0.2%Ag rolled alloy samples

A Pb−0.2%Ag rolled alloy (Kunming Hendera Science and Technology Co., Ltd., China) and a pure aluminum (>99.95%) sheet were used as the main raw materials. The process for preparation of the Al/Pb−0.2%Ag rolled-alloy samples consisted of several steps: 1) Pure aluminum sheet with a certain thickness and size was pretreated by the surface polished and embossed processing; 2) The embossed aluminum sheet undergoes heat treatment for 20 min at 200 °C as well as the vertical cast-iron mold was preheated; 3) The Pb−0.2%Ag alloy melt was obtained at 600 °C, and the previous heat-treated aluminum sheet was fixed on the vertical cast-iron mold; 4) Pb−0.2%Ag alloy melt was poured into the vertical cast-iron mold, after solidification, the composite casting plate was taken out for hot rolling and used different cooling ways (ice salt cooling, common water cooling and air cooling at room temperature); 5) After sufficient cooling, the alloy were cut into many small 1 cm × 1 cm × 1 cm pieces and 5 cm × 1 cm × 1 cm strips. The pieces were connected to a plastic isolated copper wire and cast in a denture base resin (type II, Dental Materials Factory of Shanghai Medical Instruments Co., Ltd., China) with a working area of 1.0 cm^2. A schematic of the experimental Pb−0.2%Ag rolled-alloy samples is shown in Fig. 1. The rolled-alloy pieces were used in electrochemical tests. The rolled-alloy strips were used in yield strength and Vickers hardness tests. Table 1 presents the experimental samples. The schematic of composite casting process is shown in Fig. 2.

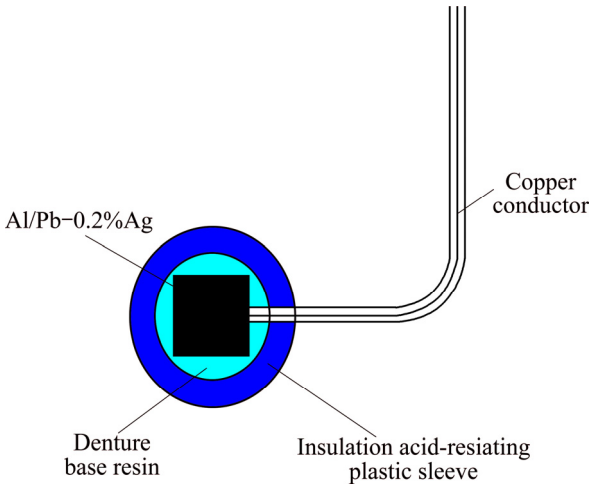

Fig. 1 Schematic diagram for Al/Pb−0.2%Ag rolled alloy experimental samples

Table 1 Experimental samples used in this research

Sample No.	Sample type
1	Al/Pb−0.2% Ag rolled alloy (cooled by ice salt cooling)
2	Al/Pb−0.2% Ag rolled alloy (cooled by common water cooling)
3	Al/Pb−0.2% Ag rolled alloy (cooled by air cooling at room temperature)

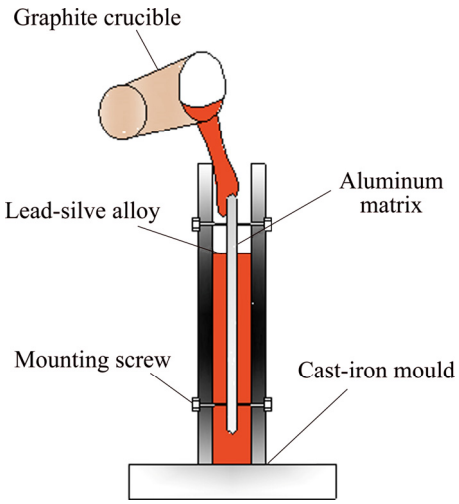

Fig. 2 Schematic diagram of composite casting process

2.2 Measurements

In this experiment, the microscopic morphology and grain size of the cross section for different samples were observed by metallographic microscope (DHV-1000, Shanghai Cikong Optical Instrument Co., Ltd., China) and electron backscatter diffraction (EBSD, Bruker Cry, Germany), respectively. The Vickers hardness measuring instrument (HV-5, Shanghai Testo Electronics Co., Ltd., China) and tensile testing machine (AG-IS, Shimadzu

Corporation, Japan) were employed to measure the Vickers hardness and yield strength of alloy samples, respectively. The sample preparation of metallography test and Vickers hardness test are as follows: first, the surface was polished, ground with 600, 1000, 1200 and 1500 soft grit SiC paper, respectively, and then ground in acetic acid and hydrogen peroxide (volume ratio of 3:1) solution, finally, polished in aluminium oxide solution (3% to 5%).

An electrochemical workstation (CS350, Corrtest, China) with three electrode systems was used in the electrochemical test, potentiodynamic curves and electrochemical impedance spectroscopy curves in a synthetic electrolyte of 50 g/L Zn^{2+} and 150 g/L H_2SO_4 at 35 °C and at an anodic current density of 500 A/m^2 (0.05 A/cm^2). Cyclic voltammetry analysis was performed in the −1.4 V to +1.7 V (MSE) potential range at a sweep rate of 20 mV/s. Anodic polarization curves were obtained at a constant scan rate of 0.5 mV/s, from an initial potential of 1.1 V (MSE) to a final potential of 1.9 V (MSE). Samples 1, 2 and 3 with the working areas 1.0 cm^2 were used as the working electrode (WE), the reference electrode (RE) was a mercurous sulfate electrode (MSE) consisting of Hg and Hg_2SO_4/sat.K_2SO_4, whereas the counter electrode (CE) was a platinum plate with the working area of 6 cm^2. The working electrode and counter electrode were connected with saturated K_2SO_4 agar salt bridge. The zinc electrowinning used in the electrochemical experiment was prepared using H_2SO_4 (analytical grade), $ZnSO_4{\cdot}7H_2O$ (analytical grade) and distilled water.

3 Results and discussion

3.1 Cross section morphology of different samples

The metallographic photos of the cross section of different Al/Pb−0.2%Ag rolled-alloy samples are shown in Fig. 3.

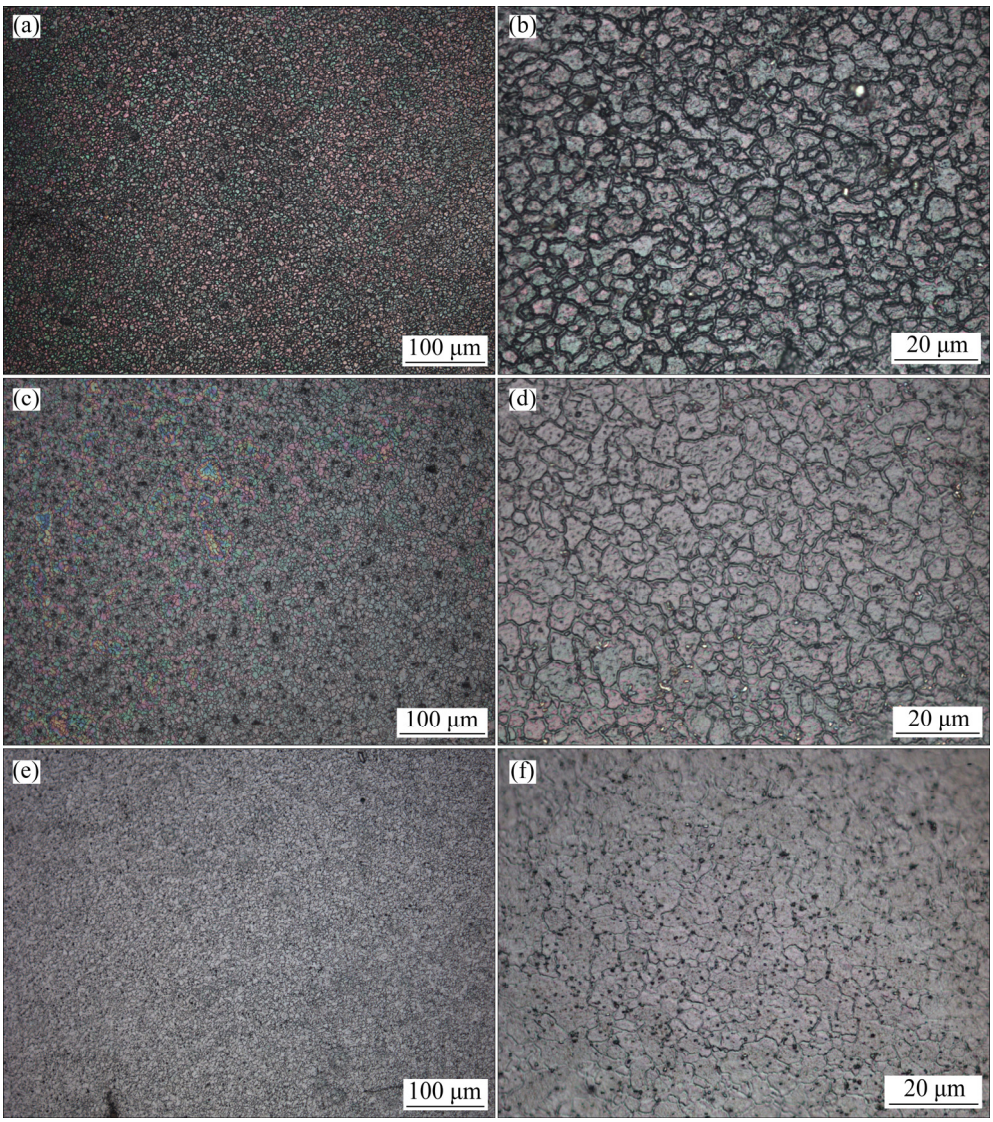

Fig. 3 Metallographic of different cooling ways for Al/Pb−0.2%Ag rolled-alloy samples: (a, b) Sample 1; (c, d) Sample 2; (e, f) Sample 3

Figures 3(a), (c) and (e) show that the morphology of different alloy samples is consisted of many irregular cellular structure, however, Figs. 3(b), (d) and (f) show that the cross section morphology changes significantly with different cooling ways. In addition, the grain size and roughness of anodic surface mainly exhibits a decreasing trend with the increase of cooling intensity. Sample 1 (ice salt cooling) exhibits the finest grain size and the thickest grain boundary. The results of electron backscatter diffraction (EBSD) detection analysis shown that the average grain size (ten grain) of Sample 1, 2 and 3 is about 50, 300 and 900 μm (±0.5 μm), respectively. In general, the smaller grain size of alloy corresponding to the greater hardness of alloy [24]. Therefore, accelerating cooling can reach the purpose of improving the mechanical strength of alloy.

3.2 Mechanical properties analysis of Al/Pb−0.2%Ag rolled alloy samples

Vickers hardness and yield strength were used to characterize the mechanical properties of the different alloy specimens in this experiment. The Vickers hardness of different rolled alloy samples can be calculated according to Eq. (1).

$$H=\frac{2F}{d^2}\times\sin\frac{136^\circ}{2}=1.8544\times\frac{F}{d^2} \quad (1)$$

where H and F represent the Vickers hardness and test force, respectively, and d represents the arithmetic mean of the indentation diagonals d_1 and d_2. In the experiment, the test force was 0.098 N. Test loading time 10 s, retention time 15 s. Before the Vickers hardness test, the alloy samples were polishing first to prevent measurement error caused by the surface oxidation. A sample was tested for 5 times and their average value was taken. The test results are listed in Table 2.

Table 2 Vickers hardness of different Al/Pb−0.2%Ag rolled alloy samples

Sample No.	Test times					Hardness (HV)
	1	2	3	4	5	
1	31.18	31.68	31.25	31.62	31.43	31.432
2	30.39	30.83	30.98	30.52	30.58	30.66
3	23.22	23.52	23.91	23.79	23.45	23.578

As shown in Table 2, Sample 1 (cooled by ice salt cooling) exhibits the largest micro-hardness (HV 31.432), whereas Sample 3 (cooled by air cooling at temperature) shows the smallest micro-hardness (HV 23.578). The results indicate that accelerated cooling increased the micro-hardness of alloy. This conclusion is in agreement with the results of metallographic analysis. The results of tensile tests are listed in Table 3.

Table 3 Yield strength and elongation of different Al/Pb−0.2%Ag rolled alloy samples

Sample No.	Yield strength/MPa	Elongation/%
1	28.43	38.67
2	28.21	40.33
3	27.08	41.33

As shown in Table 3, Sample 1 performs the largest yield strength (28.43 MPa) and the smallest elongation (38.67%). In addition, the yield strength and elongation exhibits an increasing trend with the increase of cooling intensity. The results show that accelerated cooling rate improves the ability of Al/Pb−0.2%Ag rolled alloy to resist deformation. In summary, accelerating cooling rate enhances the mechanical properties of Al/Pb−0.2%Ag rolled alloy.

3.3 CV analysis of different Al/Pb−0.2%Ag rolled alloy samples

The cyclic voltammograms of different Al/Pb−0.2%Ag rolled alloy samples are shown in Fig. 4.

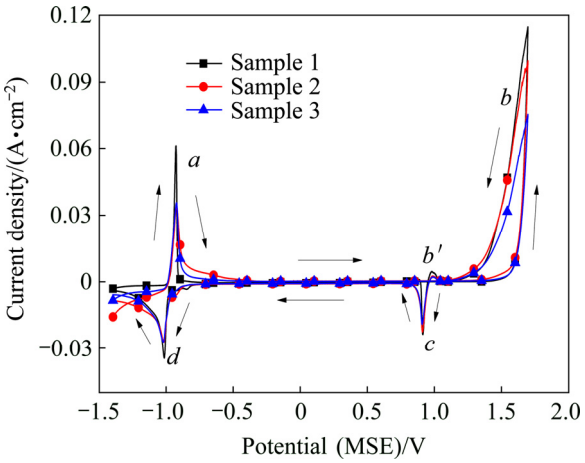

Fig. 4 Cyclic voltammograms for different Al/Pb−0.2%Ag rolled alloy anode samples

As shown in Fig. 4, all Al/Pb−0.2%Ag rolled alloy samples show that the two typical anodic (*a* and *b*) and cathodic (*c* and *d*) peaks [3,25]. The first redox peaks *a* and *d* represent the exchange reaction of Pb and $PbSO_4$. As shown in Fig. 3, Sample 1 has the smallest grain size, it will increase the area of the anode/electrolyte interface, therefore it shows the highest peak current of the peak of *a* and *d*. The cathodic peak *b* is due to the reaction $PbO\rightarrow\alpha\text{-}PbO_2$, $PbSO_4\rightarrow\beta\text{-}PbO_2$ and the oxygen evolution reaction. The molar volume of $PbSO_4$ and PbO_2 are 48 cm^3/mol and 25 cm^3/mol, respectively. In the process of the formation of PbO_2, membrane layer volume become small, and the specific surface area increased. In addition, Sample 1 has the smallest grain

size, so it shows the best oxygen evolution activity. The cathodic peak *c* corresponds to the α-PbO_2, β-PbO_2→ $PbSO_4$ reaction. Most characteristic is the appearance of a new anodic peak, *b*', at 1.0 V (MSE) during the negative direction. It is due to the oxidation of Pb to $PbSO_4$ through the pores of PbO_2, it appears only in the presence of already formed PbO_2 at positive direction [25]. As shown in Fig. 4, the peaks potential of different Al/Pb−0.2%Ag rolled alloy samples remained at a stable value. The results demonstrate that different cooling ways have no effect on reaction mechanism of the alloy anode surface [26]. However, the peaks current density of Sample 1 is higher than those of Samples 2 and 3, which means that the electrode surface reaction speed of Sample 1 is fast.

3.4 LSV analysis of different Al/Pb−0.2%Ag rolled alloy samples

The anodic polarization curves for different Al/Pb−0.2%Ag rolled alloy samples are shown in Fig. 5.

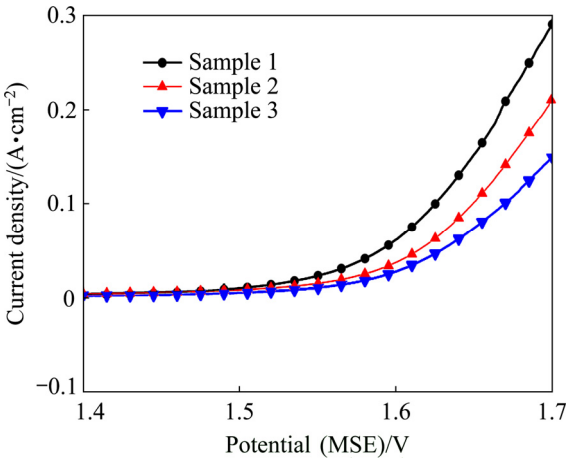

Fig. 5 Anodic polarization curves of different Al/Pb−0.2%Ag rolled alloy samples

Figure 5 shows that the oxygen evolution potential of Al/Pb−0.2%Ag rolled-alloy anodes decreased with accelerated cooling. Sample 3 presents the highest potential (1.6288V) of oxygen evolution whereas Sample 1 shows the lowest (1.5902 V) at a current density of 500 A/m^2 (0.05 A/cm^2).

According to the Tafel equation ($\eta=a+b\lg J$), where η is over-potential of oxygen evolution reaction, *a* is the Tafel constant, *b* is the Tafel slope and *J* is electrode surface current density, the over-potential (η) was calculated by using the following formula [27]: $\eta=E+0.640-1.242$, where *E* (MSE) is the potential of oxygen evolution of the anodic polarization curve, 0.640 V (SHE) is the potential of the MSE, 1.242 V is potential of oxygen evolution in a synthetic zinc electrowinning electrolyte of 50 g/L Zn^{2+} and 150 g/L H_2SO_4 at 35 °C. Therefore, the curve of η (*y*-axis) and lg*J* (*x*-axis) is drawn, *a* and *b* can be acquired by the liner fitting for relationship curve of η and lg*J* in our research (Fig. 6). Finally, the exchange current density of electrode surface, J_0, can be calculated by Tafel equation when η=0. According to the corresponding references [28,29], a_1 and b_1 corresponding to low potential area, however, a_2 and b_2 correspond to high potential area. Due to the zinc electrowinning was conducted at a current density of 500 A/m^2 (0.05 A/cm^2), in this work, the over-potential (η) and the exchange current density of electrode surface (J_0) were calculated in low potential area.

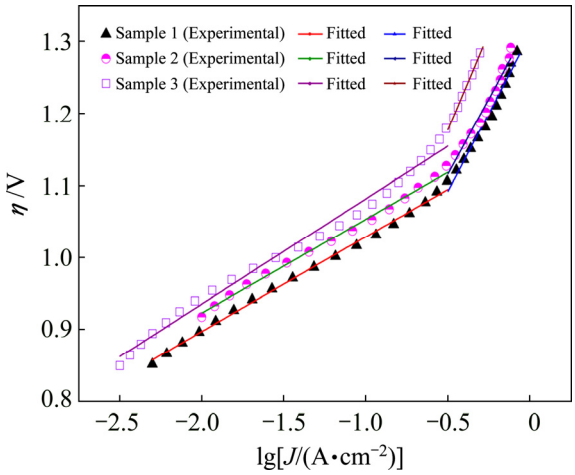

Fig. 6 Fitted Tafel lines

The kinetic parameters of oxygen evolution were calculated using Tafel equation and are listed in Table 4.

Table 4 Kinetic parameters of oxygen evolution for Al/Pb−0.2%Ag rolled alloy samples

Sample No.	a_1	b_1	a_2	b_2	J_0/(A·cm^{-2})
1	1.1604	0.1317	1.3095	0.4356	1.545×10^{-9}
2	1.1837	0.1306	1.3256	0.4199	8.639×10^{-10}
3	1.228	0.1464	1.4459	0.5366	4.093×10^{-9}

As shown in Table 4, a_1, b_1, a_2 and b_2 show an decreasing trend with accelerated cooling. Sample 1 shows the lowest a_1, b_1, a_2 and b_2 values, which can be accounted for its high roughness. The values of *a* and *b* represent the levels of cell voltage and anodic over-potential, respectively. Smaller values of *a* and *b* correspond to lower energy consumption. However, J_0 increases at first then decreases with accelerated cooling. The exchange current density, J_0, measures the reversibility of electrode reaction, and the degree of difficulty of the reaction takes place; higher exchange current density showed that the electrode is not easy to

be polarized, electrode reversibility is improved, and electrode reaction readily occurs [27].

3.5 Potentiodynamic analysis of Al/Pb−0.2%Ag rolled alloy samples

The potentiodynamic curves for different Al/Pb−0.2%Ag rolled alloy samples are shown in Fig. 7. These curves were obtained at a constant scan rate of 0.1 mV/s, from an initial potential of −1.4 V (MSE) to a final potential of −0.6 V (MSE).

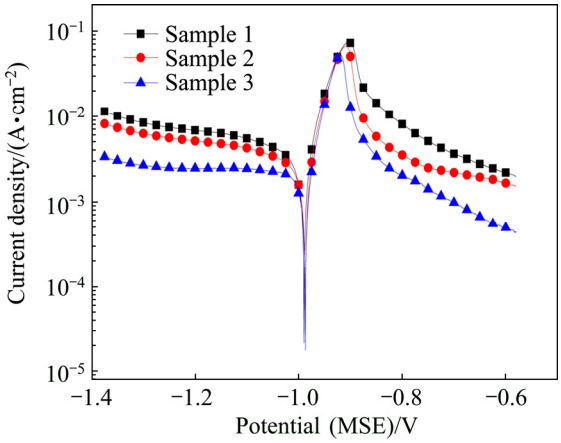

Fig. 7 Potentiodynamic curves of different cooling ways for Al/Pb−0.2%Ag rolled alloy samples

The values of self-corrosion potential, φ_{corr}, and self-corrosion current density, J_{corr}, of anode samples obtained from Fig. 7 are listed in Table 5.

Table 5 Self-corrosion potential and current density of different cooling ways for Al/Pb−0.2%Ag rolled alloy anodes

Sample No.	φ_{corr}/V	J_{corr}/(A·cm^{-2})
1	−0.987	4.38×10^{-3}
2	−0.987	3.34×10^{-3}
3	−0.989	2.29×10^{-3}

Based on Faraday's law, the relationship between self-corrosion current density and metal self-corrosion rate is expressed as follows:

$$v=\frac{MJ_{corr}}{nF} \quad (2)$$

where v, J_{corr}, M, n and F represent the corrosion rate, the corrosion current density, the metal molar mass, the metal valence and the Faraday constant, respectively. In theory, the corrosion current density, J_{corr}, is proportional to the corrosion rate ,v. However, it does not represent corrosion rate of the anodes in the electrowinning process (at high current density).

As shown in Table 5, Sample 1 shows the highest (4.38×10^{-3} A/cm^2) J_{corr} value and Sample 3 presents the lowest (2.29×10^{-3} A/cm^2) J_{corr} value. It can be seen from Eq. (2) that the corrosion rate of Sample 1 was the highest and that of Sample 3 was the lowest. The results imply that accelerated cooling decreases the corrosion resistance of Al/Pb−0.2%Ag rolled alloy at the self-corrosion potential. It may be due to that Sample 1 has the smallest grain size and the largest specific surface area, which promotes the contact between the anode and electrolyte, and then causes the alloy corrosion. It may also because the silver atoms were clustered at the grain boundaries, causing the different corrosion potential between the grain internal and the grain boundaries, so there is a corrosion potential difference between them and resulted the alloy corrosion [30]. Accelerated cooling refines the grain size as well as increases the grain boundaries area, which results the amount of galvanic cell between grain internal and grain boundaries increases and then accelerates the Al/Pb−0.2%Ag rolled alloy corrosion.

3.6 EIS analysis of different alloy samples

EIS measurements were performed by applying an AC amplitude of 5 mV root mean square over the 10^5 to 10^{-1} Hz frequency range. The applied anodic potential was 1.4 V (MSE). The results were analyzed without considering inductance using ZView 2.0 software and are shown in Fig. 8.

An equivalent circuit (Fig. 9) was proposed to simulate the electrochemical process of oxygen evolution reaction [3].

In the equivalent circuit, R_s represents the electrolyte resistance between the reference and working electrodes, R_t represents the charge transfer resistance in the electrochemical process, and C_{dl} represents the double-layer capacitance. The best-fit values for the equivalent circuit of different anode samples are listed in Table 6.

As shown in Fig. 8, the experimental (spots) and simulated (lines) data of all the Al/Pb−0.2% Ag rolled alloy can reach a good agreement. And the λ^2 values of equivalent circuit are about 10^{-4}. Form Table 6, with the accelerated cooling, the charge-transfer resistance, R_t, decreased, whereas C_{dl} exhibits an increasing trend. Compared with Samples 2 and 3, Sample 1 shows the lowest R_t. As we know, the smaller charge transfer resistance means that the electrode reaction more easily occurs. Therefore, the results indicate that accelerated cooling can improve the electrochemical activity of Al/Pb−0.2%Ag rolled alloy. However, the increased C_{dl} values may be due to the anodic surface that adsorbed more intermediate product, such as HSO_4^-/SO_4^{2-}, during the polarization process [31].

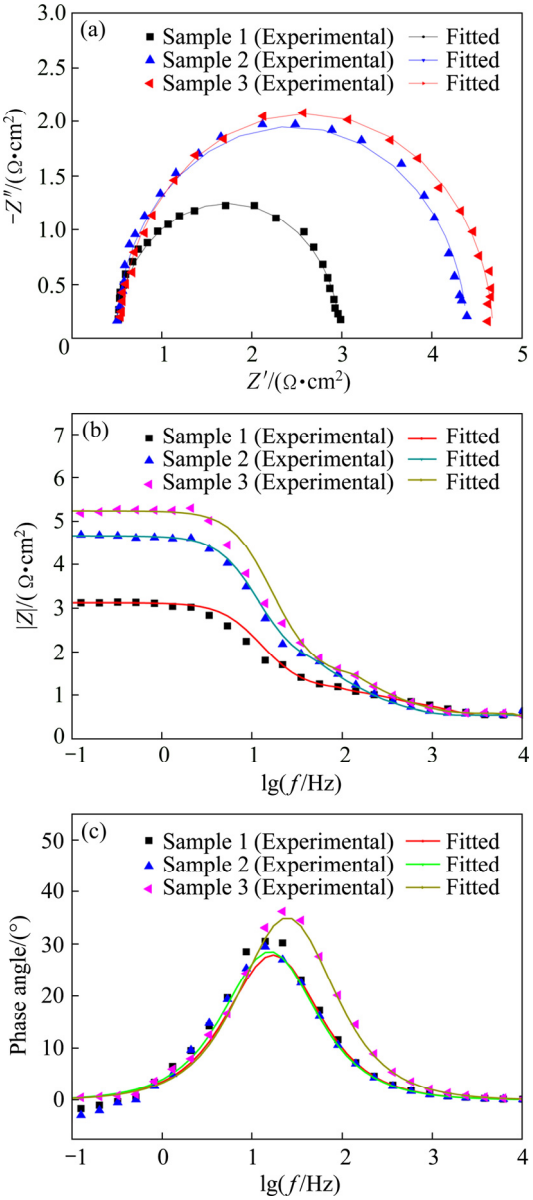

Fig. 8 EIS of different cooling ways for Al/Pb−0.2%Ag rolled alloy anodes: (a) Nyquist plots; (b, c) Bolt plots

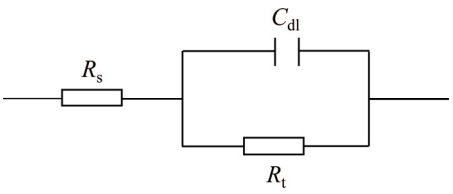

Fig. 9 Electrical equivalent circuit used to simulate impedance data

Table 6 Best-fit values for equivalent circuit

Sample No.	$R_s/(\Omega\cdot cm^2)$	$C_{dl}/(F\cdot cm^{-2})$	$R_t/(\Omega\cdot cm^2)$
1	0.4837	4.367×10^{-3}	2.455
2	0.4938	3.846×10^{-3}	3.893
3	0.5387	2.751×10^{-3}	4.135

4 Conclusions

1) Accelerated cooling not only improves the mechanical properties and the electrochemical activity, but also decreases the oxygen evolution potential and the charge transfer resistance of Al/Pb−0.2%Ag rolled alloy anode in zinc electrowinning process. This phenomenon may be caused by the roughness of anodic surface. Compared with cooled by air, the oxygen evolution potential of alloy cooled by ice salt are decreased by 38 mV under 500 A/m^2.

2) However, accelerated cooling enhances the self-corrosion rate of Al/Pb−0.2%Ag rolled alloy to some extent. It may be due to that the large specific surface area promotes the contact between the anode and electrolyte.

References

[1] ZHONG Xiao-cong, YU Xiao-ying, JIANG Liang-xing, LV Xiao-jun, LIU Fang-yang, LAI Yan-qing, LI Jie. Influence of fluoride ion on the performance of Pb−Ag anode during long-term galvanostatic electrolysis [J]. Journal of the Minerals, Metals and Materials Society, 2015, 7: 2022−2027.

[2] FELDER A, PRENGAMAN R D. Lead alloys for permanent anodes in the nonferrous metals industry [J]. Journal of the Minerals, Metals and Materials Society, 2006, 58: 28−31.

[3] ZHANG W, HOULACHI G. Electrochemical studies of the performance of different Pb−Ag anodes during and after zinc electrowinning [J]. Hydrometallurgy, 2010, 104: 129−135.

[4] MOHAMMADI M, ALFANTAZI A. The performance of Pb−MnO_2 and Pb−Ag anodes in Mn(II)-containing sulphuric acid electrolyte solutions [J]. Hydrometallurgy, 2015, 153: 134−144.

[5] MCGINNITY J J, NICOL M J. The role of silver in enhancing the electrochemical activity of lead and lead-silver alloy anodes [J]. Hydrometallurgy, 2014, 144−145: 133−139.

[6] ZHONG Shui-ping, LAI Yan-qing, JIANG Liang-xing, LV Xiao-jun, CHEN Pei-ru, LI Jie, LIU Ye-xiang. Fabrication and anodic polarization behavior of lead-based porous anodes in zinc electrowinning [J]. Journal of Central South University of Technology, 2008, 15: 757−762.

[7] ZHAN Peng, XU Rui-dong, HUANG Li-ping, CHEN Bu-ming, ZHOU Jian-feng. Effects of polyaniline on electrochemical properties of composite inert anodes used in zinc electrowinning [J]. Transactions Nonferrous Metals Society of China, 2012, 22: 1693−1700.

[8] HUANG Hui, ZHOU Ji-yu, CHEN Bu-ming, GUO Zhong-cheng. Polyaniline anode for zinc electrowinning from sulfate electrolytes [J]. Transactions Nonferrous Metals Society of China, 2010, 20: 288−292.

[9] LAI Yan-qing, LI Yuan, JIANG Liang-xing, LV Xiao-jun, LI Jie, LIU Ye-xiang. Electrochemical performance of a Pb/Pb−MnO_2 composite anode in sulfuric acid solution containing Mn^{2+} [J]. Hydrometallurgy, 2012, 115−116: 64−70.

[10] YANG Hai-tao, LIU Huan-rong, ZHANG Yong-chun, CHEN Bu-ming, GUO Zhong-cheng, XU Rui-dong. Properties of a new type Al/Pb−0.3% Ag alloy composite anode for zinc electrowinning [J]. International journal of Minerals Metallurgy and Materials, 2013, 20: 986−993.

[11] YANG Hai-tao, CHEN Bu-ming, LIU Jian-hua, GUO Zhong-cheng, ZHANG Yong-chun, XU Rui-dong. Preparation and properties of Al/Pb−Ag−Co composite anode material for zinc electrowinning [J]. Rare Metal Materials and Engineering, 2014, 43: 2889−2892.

[12] YANG Hai-tao, CHEN Bu-ming, LIU Huan-rong, GUO Zhong-cheng, ZHANG Yong-chun, LI Xue-long, XU Rui-dong. Effects of manganese nitrate concentration on the performance of an aluminum substrate β-PbO_2−MnO_2−WC−ZrO_2 composite electrode material[J]. International Journal of Hydrogen Energy, 2014, 39: 3087−3099.

[13] YANG Hai-tao, CHEN Bu-ming, GUO Zhong-cheng, LIU Huan-rong, ZHANG Yong-chun, Huang Hui, XU Rui-dong, FU Reng-chun. Effects of current density on preparation and performance of Al/conductive coating/α-PbO_2−CeO_2−TiO_2/ β-PbO_2−MnO_2−WC−ZrO_2 composite electrode materials [J]. Transactions Nonferrous Metals Society of China, 2014, 24: 3394−3404.

[14] ZHANG Yong-chun, CHEN Bu-ming, YANG Hai-tao, Huang Hui, GUO Zhong-cheng. Anodic behavior and microstructure of Al/Pb−Ag−Co anode during zinc electrowinning [J]. Journal of Central South University, 2014, 21: 83−88.

[15] ZHANG Yong-chun, CHEN Bu-ming, YANG Hai-tao, GUO Zhong-cheng, XU Rui-dong. Anodic behavior and microstructure of Al/Pb−Ag anode during zinc electrowinning [J]. Transactions Nonferrous Metals Society of China, 2014, 24: 893−899.

[16] ZHANG Yong-chun, CHEN Bu-ming, GUO Zhong-cheng. Electrochemical properties and microstructure of Al/Pb−Ag and Al/Pb−Ag−Co anodes for zinc electrowinning [J]. Acta Metallurgica Sinica-English Letters, 2014, 27: 331−337.

[17] CHEN Bu-ming, GUO Zhong-cheng, LIU Jian-hua, ZHANG Yong-chun, YANG Hai-tao. Study on the corrosion resistance of Pb−Ag−Co alloy electrodeposited on Al substrate [J]. Plating and Finishing, 2014, 36: 1−4. (in Chinese)

[18] CHANG S H, WU S K. Effect of cooling rate on transformation temperature measurements of $Ti_{50}Ni_{50}$ alloy by differential scanning calorimetry and dynamic mechanical analysis [J]. Materials Characterization, 2008, 59: 987−990.

[19] LI Shi-kai, XIONG Bai-qing, HUI Song-xiao. Effects of cooling rate on the fracture properties of TA15 ELI alloy plates [J]. Rare Metals, 2007, 26: 33−38.

[20] ZEER G M, PERVUKHIN M V, ZELENKOVA E G. Effect of cooling rate on microstructure formation during crystallization of aluminum alloy 1417M [J]. Metal Science and Heat Treatment, 2011, 53: 210−212.

[21] ZHANG Shuang-yin, LIN Xin, CHEN Jing, HUANG Wei-dong. Effect of solution temperature and cooling rate on microstructure and mechanical properties of laser solid forming Ti−6Al−4V alloy [J]. Chinese Optics Letters, 2009, 7: 498−501.

[22] YANG Lin, FENG Hui, QIU Ke-qiang, CHEN Li-jia, LIU Zheng. Effect of cooling rate on microstructure and compressive performance of AZ91 magnesium alloy [J]. Transactions of Nonferrous Metals Society of China, 2006, 16: 1698−1702.

[23] WANG Jing-feng, HUANG Song, GUO Sheng-feng, WEI Yi-yun, PAN Fu-sheng. Effects of cooling rate on microstructure, mechanical and corrosion properties of Mg−Zn−Ca alloy [J]. Transactions of Nonferrous Metals Society of China, 2013, 23: 1930−1935.

[24] HU Xiao-wu, AI Fan-rong, YAN Hong. Influences of pouring temperature and cooling rate on microstructure and mechanical properties of casting Al−Si−Cu aluminum alloy [J]. Acta Metallurgica Sinica, 2012, 25: 272−278.

[25] YANG Hai-tao, LIU Huan-rong, ZHANG Yong-chun, CHEN Bu-ming, GUO Zhong-cheng, XU Rui-dong. Cyclic voltammetric studies of the behavior of Pb−0.3%Ag−0.06%Ca rolled alloy anode during and after zinc electrowinning [J]. Advanced Materials Research, 2013, 750−752: 2232−2235.

[26] DENG Zhao-xiang, Zhao Wei, LIN Xiang-qin. Simplex optimization-numerical simulation method for fast cyclic voltammetric curve fitting [J]. Chinese Journal of Analytical Chemistry, 1999, 27: 383−387. (in Chinese)

[27] XU Rui-dong, HUANG Li-ping, ZHOU Jian-feng, ZHAN Peng, GUAN Yong-yong, KONG Ying. Effects of tungsten carbide on electrochemical properties and microstructural features of Al/Pb−PANI-WC composite inert anodes used in zinc electrowinning [J]. Hydrometallurgy, 2012, 125: 8−15.

[28] MOHAMMADI M, MOHAMMADI F, ALFANTAZI A. Electrochemical reactions on metal-matrix composite anodes for metal electrowinning [J]. Journal of the Electrochemical Society, 2013, 160: 35−43.

[29] TAGUCHI M, TAKAHASHI H, NAGAI M, AICHI T, SATO R. Characteristics of Pb-based alloy prepared by powder rolling method as an insoluble anode for zinc electrowinning [J]. Hydrometallurgy, 2013, 136: 78−84.

[30] CHEN Y Y, TZENG H J, WEI L I, WANG L H, OUNG J C, SHIH H C. Corrosion resistance and mechanical properties of low-alloy steels under atmospheric conditions [J]. Corrosion Science, 2005, 47: 1001−1021.

[31] LAI Yan-qing, LI Yuan, JIANG Liang-xing, XU Wang, LV Xiao-jun, LI Jie, LIU Ye-Xiang. Electrochemical behaviors of co-deposited Pb/Pb−MnO_2 composite anode in sulfuric acid solution-Tafel and EIS investigations [J]. Journal of Electroanalytical Chemistry, 2012, 671: 16−23.

冷却方式对电积锌用 Al/Pb−0.2%Ag 轧制合金性能的影响

周向阳[1]，王 帅[1]，杨 娟[1]，郭忠诚[2,3]，杨 健[2]，马驰原[1]，陈步明[2]

1. 中南大学 冶金与环境学院，长沙 410083；2. 昆明理工大学 冶金与能源工程学院，昆明 650093；
3. 昆明理工恒达科技股份有限公司，昆明 650106

摘 要：为了研究新型电积锌阳极材料，通过复合浇铸和热压制备了 Al/Pb−0.2%Ag 合金，并研究了冷却方式对其性能的影响。金相测试结果表明，随着冷却强度的增强，Al/Pb−0.2%Ag 轧制合金的维氏硬度和屈服强度逐渐增强。并且，通过冰盐冷却的 Al/Pb−0.2%Ag 合金呈现出最好的晶粒尺寸以及最低的析氧电位 (1.5902 V), 而通过水冷却和空气自然冷却合金的析氧电位分别为 1.6143 V 和 1.6288 V。然而，通过冰盐冷却的 Al/Pb−0.2%Ag 合金的腐蚀电流密度和腐蚀速率都达到了最高。这可能是由于其具有较大的比表面积，进而增加了阳极和电解液的接触面积。

关键词：Al/Pb−0.2%Ag 轧制合金；冷却方式；机械性能；电催化活性；耐腐蚀性；电积锌

(Edited by Yun-bin HE)